Astrocyte-Mediated Higher-Order Control of Synaptic Plasticity

Gustavo Menesse, Ana P. Millán & Joaquín J. Torres

1 Facilitation mechanism in absence of gliotransmitter release or in absence of pre-synaptic facilitation mechanism.

If there is no gliotransmitters released in a long time, means that $\Theta([Ca^{+2}]_a - Ca_{thr}) = 0$, or that all resources have been consumed $x_a^{as}(t) \approx 0$. Then $\gamma_{ija}^{as}(t) = 0$, and the release probability will be,

$$u_{ija}(\gamma_{ija}^{as} = 0, \gamma_{ij}^{pre}, t) = U_{SE} + (1 - U_{SE})\gamma_{ij}^{pre} \,, \tag{S.1}$$

taking the derivative in time we have,

$$\frac{du_{ij}(\gamma_{ij}^{pre}, t)}{dt} = U_{SE} + (1 - U_{SE})\frac{d\gamma_{ij}^{pre}}{dt} \,,$$

Substituting the dynamics of the pre-synaptic activated fraction γ_{ij}^{pre} when $\gamma_{ija}^{as} = 0$, gives

$$\frac{du_{ij}(\gamma_{ij}^{pre}, t)}{dt} = (1 - U_{SE})\left[-\frac{\gamma_{ij}^{pre}}{\tau_{pre}} + U_{SE}\left(1 - \gamma_{ij}^{pre}\right)\delta(t - t_i^{spk})\right] \,,$$

From (S.1), we can express γ_{ij}^{pre} and $(1 - \gamma_{ij}^{pre})$ as function of $u_{ij}(t)$ as

$$\begin{aligned} \gamma_{ij}^{pre}(t) &= \frac{u_{ij}(t) - U_{SE}}{1 - U_{SE}} \\ 1 - \gamma_{ij}^{pre}(t) &= \frac{1 - u_{ij}(t)}{1 - U_{SE}} \,. \end{aligned}$$

And by substituting this expressions in the $u(t)$ dynamics we obtain,

$$\frac{du_{ij}}{dt} = \frac{U_{SE} - u_{ij}(t)}{\tau_{pre}} + U_{SE}(1 - u_{ij}(t))\delta(t - t_i^{spk}) \,.$$

Which is the usual pre-synaptic short-term facilitation model [1, 2].

Otherwise, if there is no pre-synaptic spikes in a long time, the pre-synaptic activated fraction $\gamma_{ij}^{pre} = 0$, following similar reasoning's as the previous case, yields to

$$\frac{du_{ija}}{dt} = \frac{U_{SE} - u_{ija}(t)}{\tau_{as}} + G_a(t)(\varepsilon - u_{ija}(t))\Theta([Ca^{+2}]_a - Ca_{thr}) \,,$$

which is our equivalent to De Pitta model [3], where the only difference is that we have a continuous release if astrocytic cytosolic calcium concentration is above a release threshold, while De Pitta describe it as a singular event in time.

2 Neuronal clique activity and astrocytic modulation

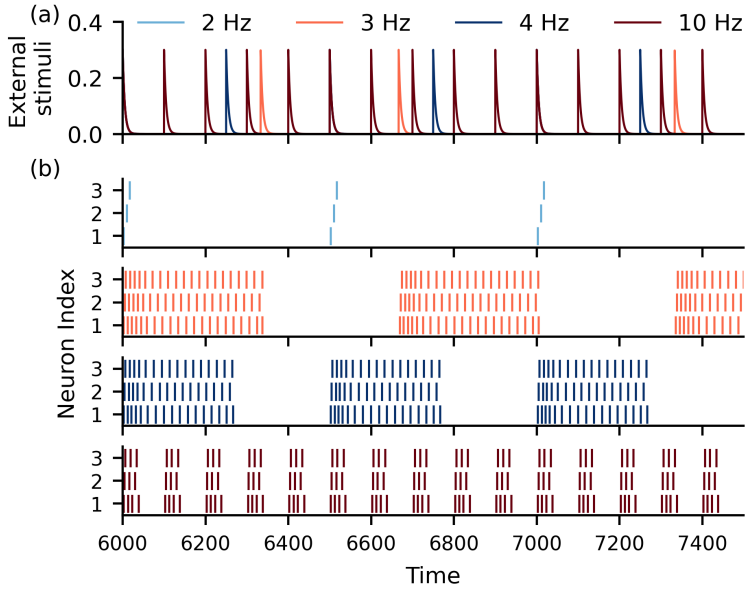

Supplementary figure A: **Network activity under different stimulation frequency in experimental scheme without gliotransmission**. For different stimulations frequency, if the synaptic current is low, the system shows different responses such as synfire activity (stimuli at 2 Hz), Up-Down states switching via external inputs (3 and 4 hz), short bursting activity (> 5 Hz). For this richness to be possible, the synaptic current should be large enough to propagate activity, but small enough to avoid run-away excitatory activity. Here, we use fraction of neurotransmitter in the synaptic cleft $\alpha = 0.5$, neurotransmitter steady-state release probablity $U_{SE} = 0.1$ and no gliotransmitter release ($U_{SE}^{as} = 0$).

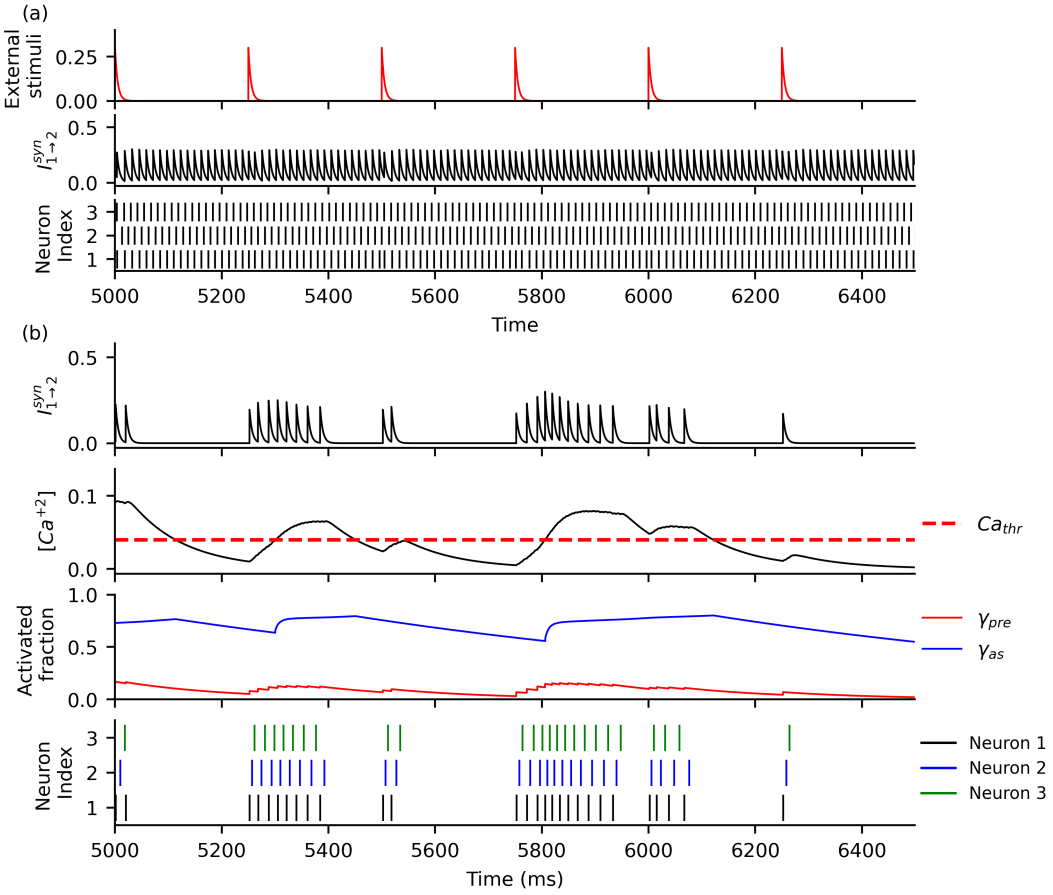

Supplementary figure B: **Gliotransmission avoid run-away activity caused by an excessive synaptic current**. **(a)** Run-away activity caused by excess of synaptic current. (a) Top panel illustrates synaptic current from external stimuli, (a) Middle panel shows synaptic current from neuron 1 to 2 and (a) Bottom panel depicts the neuronal spiking raster plot. Increasing the amount of neuroreceptors in the synaptic cleft ($\alpha = 0.8$) make the system to enter a self-sustained activity regime where the system becomes practically unresponsive to inputs. **(b)** In presence of gliotransmission, the triadic interaction modulates the synaptic facilitation, protecting the circuit against run-away excitatory activity. (b) Top panels show synaptic current $I^{syn}_{1\to 2}$ from neuron 1 to 2 and global calcium concentration $[Ca^{+2}]$ in astrocyte. (b) Bottom panels illustrate facilitation activation fractions from both pre-synaptic and astrocitic mechanism (γ_{pre} and γ_{as}) and neuronal spiking raster plot. In both cases, stimulation frequency is 4 Hz, $U_{SE} = 0.1$ and $\epsilon = 0.01$. The gliotransmission probability used was $U_S = 0$ in (a) and $U_S = 0.1$ in (b). All other parameters are shown in Table 1.

3 Safe regime vs self-sustained activity (SSA) regime.

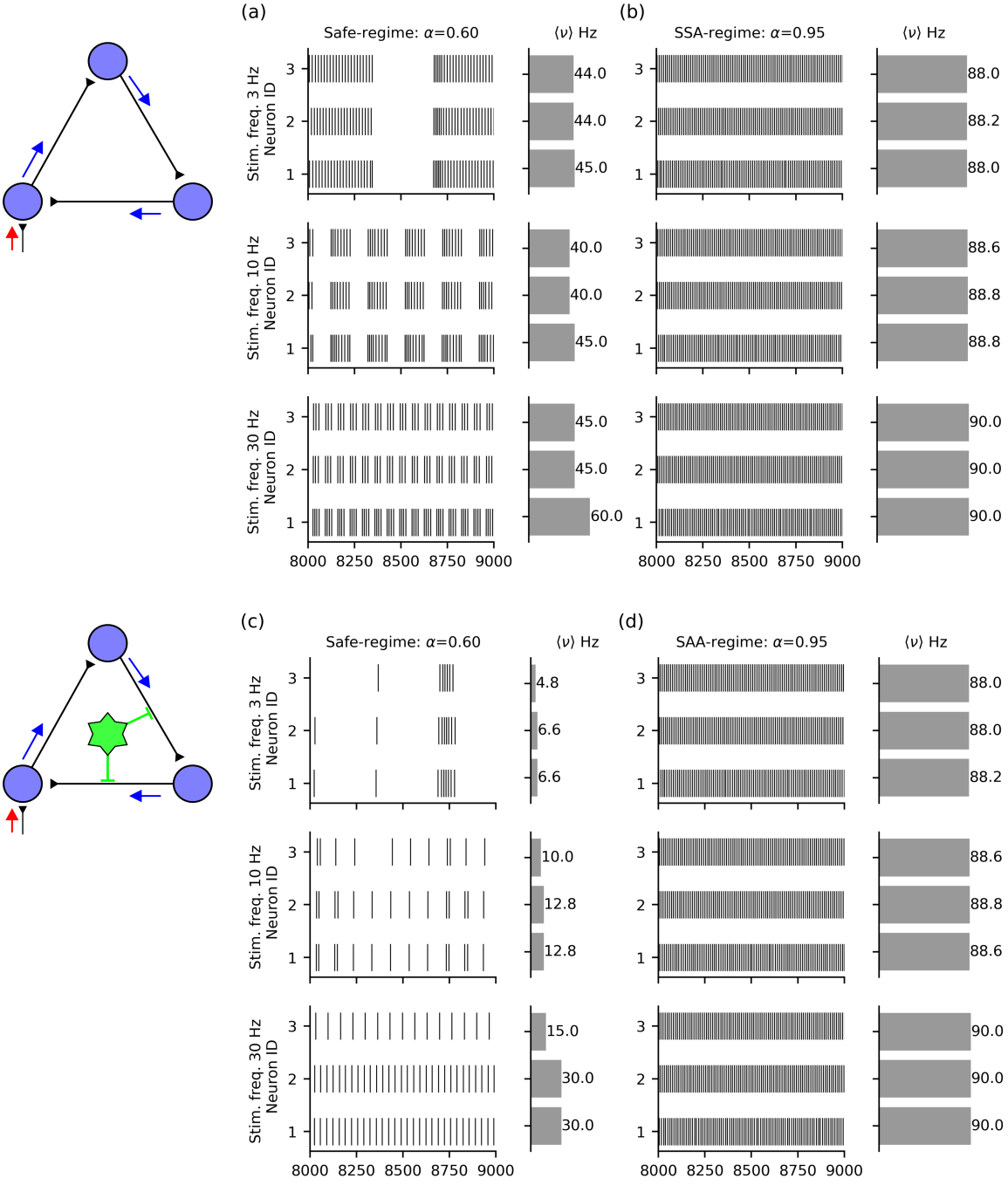

Supplementary figure C: **Raster plots and average firing rates in safe vs. self-sustained activity regimes under different stimulus frequencies.** Each panel shows the spike raster (left) and average firing rates (right) for all neurons. (a) In the safe regime ($\alpha = 0.6$), without astrocyte modulation, the circuit exhibits up–down state switching driven by external input (as in Figure A). Neurons show weak, irregular average firing rate responses to stimulus frequency. (b-d) In the SSA regime, the circuits becomes insensitive to external input, maintaining high firing rates with minimal variation. (c) In the safe regime, with astrocytic modulation, the circuit exhibits strong, frequency-dependent responses, with average firing rates increasing monotonically with stimulus frequency.

4 Minimum amplitude of synaptic current to propagate activity

To identify the SSA regime more accurately, we will derive some expressions for the minimal amplitude of synaptic current that, given a specific time and value of membrane potential of the post-synaptic neuron, will generate a spike. If all synaptic current amplitude measured in a given simulation are above this value, means that even if external stimuli stops, the system will maintain activity in a self-sustained manner.

The membrane potential and the synaptic current dynamics are described as,

$$\begin{aligned} \tau_v \frac{dV(t)}{dt} &= -V(t) + RA_{se}y(t) \\ \frac{dy(t)}{dt} &= -\frac{1}{\tau_{in}}y(t) + \alpha x U \delta(t^{spk} - t) \end{aligned}$$

Where R is the membrane resistence, C is the membrane capacitance and $\tau_v = RC$. A_{se} is the maximum current amplitude, $y(t)$ is the fraction of activated neurotransmitters, α is the fraction of neurotransmitters that stay in the synaptic cleft, xU is the synaptic efficacy and τ_{in} is the synaptic current time scale.

After a spike at time $t^{spk} = 0$ in the pre-synaptic neuron, the fraction of activated neurotransmitter follows

$$y(t) = (\alpha x U + y(0))\, e^{-\frac{t}{\tau_{in}}}$$

Therefore, the change in membrane potential after this event can be computed,

$$\frac{dV(t)}{dt} = -\frac{1}{\tau_v}V(t) + \frac{RA_{se}}{\tau_v}\left[(\alpha x U + y(0))\, e^{-\frac{t}{\tau_{in}}}\right]$$

Solving, we obtain,

$$V(t) = \frac{RA_{se}\,(\alpha x U + y(0))\,\tau_{in}}{\tau_{in} - \tau_v}\left[e^{-\frac{t}{\tau_{in}}} - e^{-\frac{t}{\tau_v}}\right] + V(0)e^{-\frac{t}{\tau_v}}$$

For the synaptic current to be capable of generating a spike in the neuron, the maximum of $V(t)$ should be equal or greater than the threshold V_{thr}.

The time were the membrane potential will achieve it's maximum value is easily computed finding the extreme of the last equation. This time is,

$$t_{max} = \frac{\tau_v \tau_{in}}{\tau_{in} - \tau_v} \ln\left\{\frac{1}{\tau_v}\left[\tau_{in} - \frac{V(0)(\tau_{in} - \tau_v)}{RA_{se}\,(\alpha x U + y(0))}\right]\right\}$$

To simplify notation we use $C = \frac{1}{\tau_v}\left[\tau_{in} - \frac{V(0)(\tau_{in}-\tau_v)}{RA_{se}(\alpha x U + y(0))}\right]$.

The maximum value of membrane potential is,

$$V_{max} = \left(\frac{\tau_{in}}{\tau_v - \tau_{in}}\right) RA_{se}\,(\alpha x U + y(0))\left[C^{\frac{\tau_v}{\tau_v - \tau_{in}}} - C^{\frac{\tau_{in}}{\tau_v - \tau_{in}}}\right] + V(0)C^{\frac{\tau_{in}}{\tau_v - \tau_{in}}}$$

The synaptic current will generate a spike only if $V_{max} \geq V_{thr}$, therefore given a $y(0)$ and $V(0)$, a spike will be generate if the following inequality holds,

$$\left(\frac{\tau_{in}}{\tau_v - \tau_{in}}\right) RA_{se}\,(\alpha x U + y(0))\left[C^{\frac{\tau_v}{\tau_v - \tau_{in}}} - C^{\frac{\tau_{in}}{-\tau_{in} - \tau_v}}\right] + V(0)C^{\frac{\tau_{in}}{\tau_v - \tau_{in}}} \geq V_{thr} \tag{S.2}$$

Importantly, if the spike occurs while the post-synaptic neuron is in the refractory period, we need to compute the synaptic current $y(t)$ at instant t when the post-synaptic neuron exits the refractory period.

In the case of rest membrane value $V(0) = 0$ and pre-spike synaptic current $y(0) = 0$ the expression simplifies to,

$$\alpha x U \underbrace{\left(\frac{RA_{se}\tau_{in}}{\tau_v - \tau_{in}}\right)\left[\left(\frac{\tau_{in}}{\tau_v}\right)^{\frac{\tau_v}{\tau_{in} - \tau_v}} - \left(\frac{\tau_{in}}{\tau_v}\right)^{\frac{\tau_{in}}{\tau_{in} - \tau_v}}\right]}_{B} - V_{thr} \geq 0$$

$$\alpha x U \geq \frac{V_{thr}}{B}$$

Therefore, we can compute the minimum value of activated fraction amplitude $\alpha x U$ to produce a spike. If astrocytic modulation reduce the release probability U, then a larger value of α will be needed to produce a transition to SSA regime.

4.1 Calculation of SSA transition line

From the previous analysis, we know how it should be the synaptic current arriving to a post-synaptic neuron to induce a spike. If all synaptic currents in the system satisfy the condition given in Eq. S.2, then every emitted spike will reliably trigger a spike in a postsynaptic partner. In this case, each spike induces another, perpetuating activity throughout the network and leading to a self-sustained activity (SSA) regime.

To compute the transition line shown in Figure 2 of the main text, we recorded, during simulation, the exact arrival time of spikes at each neuron, along with the corresponding state of the activated fraction $y(t)$, the membrane potential $V(t)$ at the time of spike arrival ($t = 0$), and the values of the plasticity variables U and x. We then evaluated whether the inequality in Eq. S.2 was satisfied for all spike events in the simulation. If this condition holds for all recorded spikes, it indicates that network activity can be sustained even after external stimulation is removed—thus, the system is in the SSA regime.

We validated this criterion by running simulations with α values slightly above and below the computed SSA transition line. After removing the external stimulation, we observed that activity persisted for α above the line and ceased for α below it (not shown), in agreement with the predicted SSA transition.

5 Modulation of different synapses in the circuit.

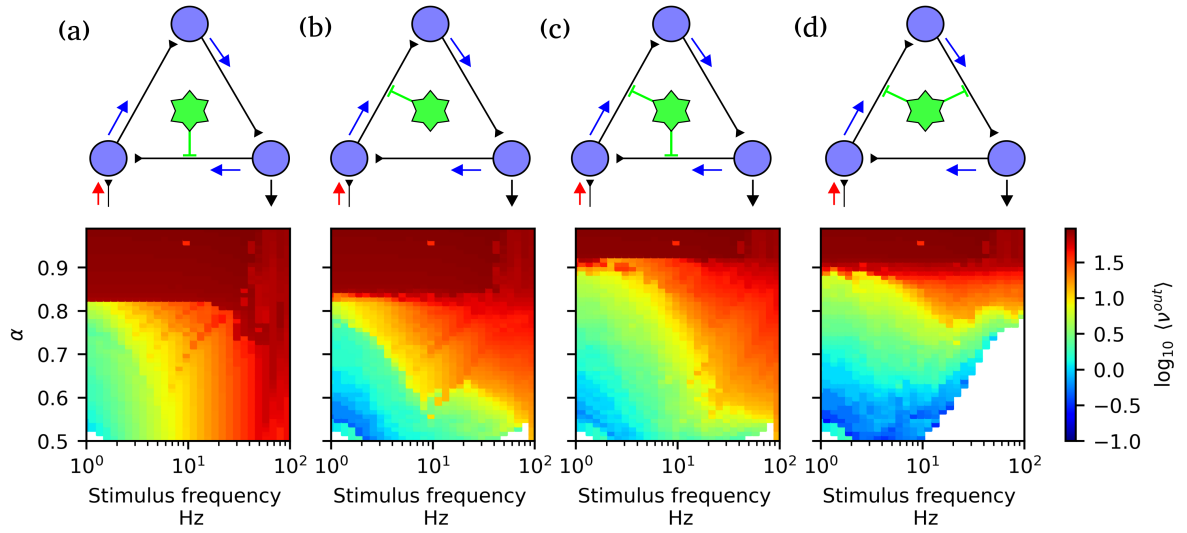

Supplementary figure D: **Astrocyte modulation of the first synapse disrupt activity propagation to read-out neuron at high frequencies.** We show network activity through the average firing frequency of the read-out neuron (indicated by a black arrow in the graph diagrams) $\langle\nu^{out}\rangle$. (a) Only the last synapse (recurrence synapse) is modulated by Astrocyte. (b-d) When the first synapse is modulated, we can see activity in the read-out neuron is disrupted (white region) for small values of α ($\alpha < 0.6$ in panels b-c and $\alpha < 0.75$ in d) and high-frequency stimulus (> 50 Hz in b-c and > 10 Hz in d). All other details are as in Figure 1 of the main text. Parameters: $\varepsilon = 0.01$, $\mathrm{Ca}_{th} = 0.04$, $\beta = 0.05$. Other simulation parameters are listed in Table 1.

6 Dynamic range under different modulation schemes

Introducing random spike train allow us to have smother transfer functions as the average firing rate presents less abrupt changes with order parameter α and stimulus frequency. Therefore, for the estimation of the dynamic range all simulations where done using Poisson spike train as input instead of periodic spike trains. As shown in Figure E, the circuit present qualitatively similar behavior for random stimulus than for periodic ones.

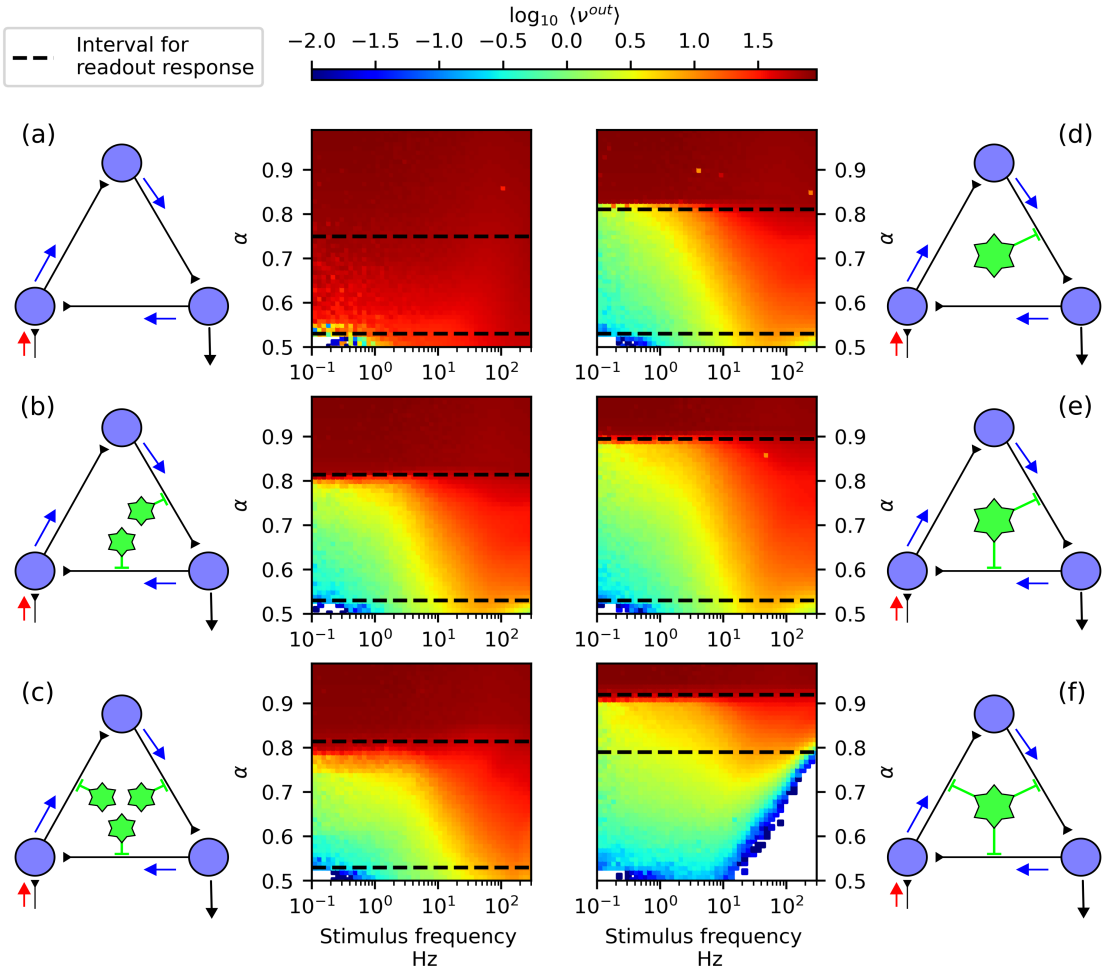

Supplementary figure E: **Circuit response to Poisson spike train present the similar qualitative features than for periodic spike train.** Here the stimulus is define as Poisson spike train instead of periodic stimulus (as main text). We show network activity through the average firing frequency of the read-out neuron (indicated by a black arrow in the graph diagrams) $\langle \nu^{out} \rangle$. All other details are as in Figure 1 of the main text. The region between the black dashed lines indicates the range of α values for which the read-out neuron responds to the stimulus (below SSA transition) across the explored range of stimulation frequencies. Parameters: $\varepsilon = 0.01$, $Ca_{th} = 0.04$, $\beta = 0.05$. Other simulation parameters are listed in Table 1.

To estimate the dynamical range we will follow a simple, but standard strategy. From the simulated activity of read-out neuron, we first obtain the minimum and maximum response firing rate F_{min} and F_{max}, where F_{min} is the response observed at the minimal stimulus used 0.1Hz, and F_{max} is the response observed at 200 Hz stimulus firing rate, which give us an approximation to the saturation frequency of the circuit. Next, we define an arbitrary interval of response between 5% and 95% percent of the full response interval. This choice will not affect our result as is fixed for all situations we are comparing here. Now we identified at which stimulus frequency we obtain $F_{0.05}$ and $F_{0.95}$, it means, $S_{0.05}$ and $S_{0.95}$ and finally, we define the dynamical range as $\Delta = 10 \log_{10} (S_{0.95}/S_{0.05})$. All elements of this calculation are shown in scheme presented in Figure F.

This definition of dynamical range is clearly applicable when the response transfer function (response function) is monotonically increasing. However, we will use the definition for our response even when the data does not shown a clear monotonicity, in this cases, we will see negative values or inconsistent values of Δ, meaning Δ change abruptly with the parameter α.

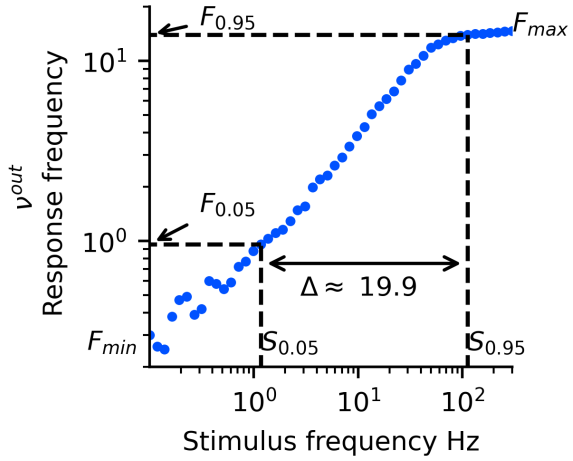

Supplementary figure F: **Dynamical range estimation.** From measurements of firing rate of read-out neuron for a range of stimulus frequency we estimate the dynamical range of the circuit in dB as $\Delta = 10 \log_{10}(S_{0.95}/S_{0.05})$, where S_x is the stimulus frequency at which the read-out neuron firing rate is $F_x = F_{min} + x\,(F_{max} - F_{min})$.

The results of the dynamical range estimation for different astrocytic modulation schemes and range of parameter α is presented in Figure G. We can see that the dynamical range show a positive and consistent behavior (blue circles in Figure G) for values of α below the transition to the self-sustained activity regime (SAA) (indicated with dashed black lines). This regimes is what we call monotonic positive regime, as the read-out neuron response by consistently increasing it's firing rate with the increase on stimulus frequency.

In absence of astrocytic modulation, as the network is more susceptible to the SAA regime, we see that there is a small range of values α where the network present a positive and consistent dynamical range. The introduction of astrocytic modulation of the synaptic plasticity mechanism dramatically spans the range of α where a clear consistent monotonic positive response is observed. This range is maximal in the high-order modulation scheme (see Figure G.e), where only internal synapses are being modulated.

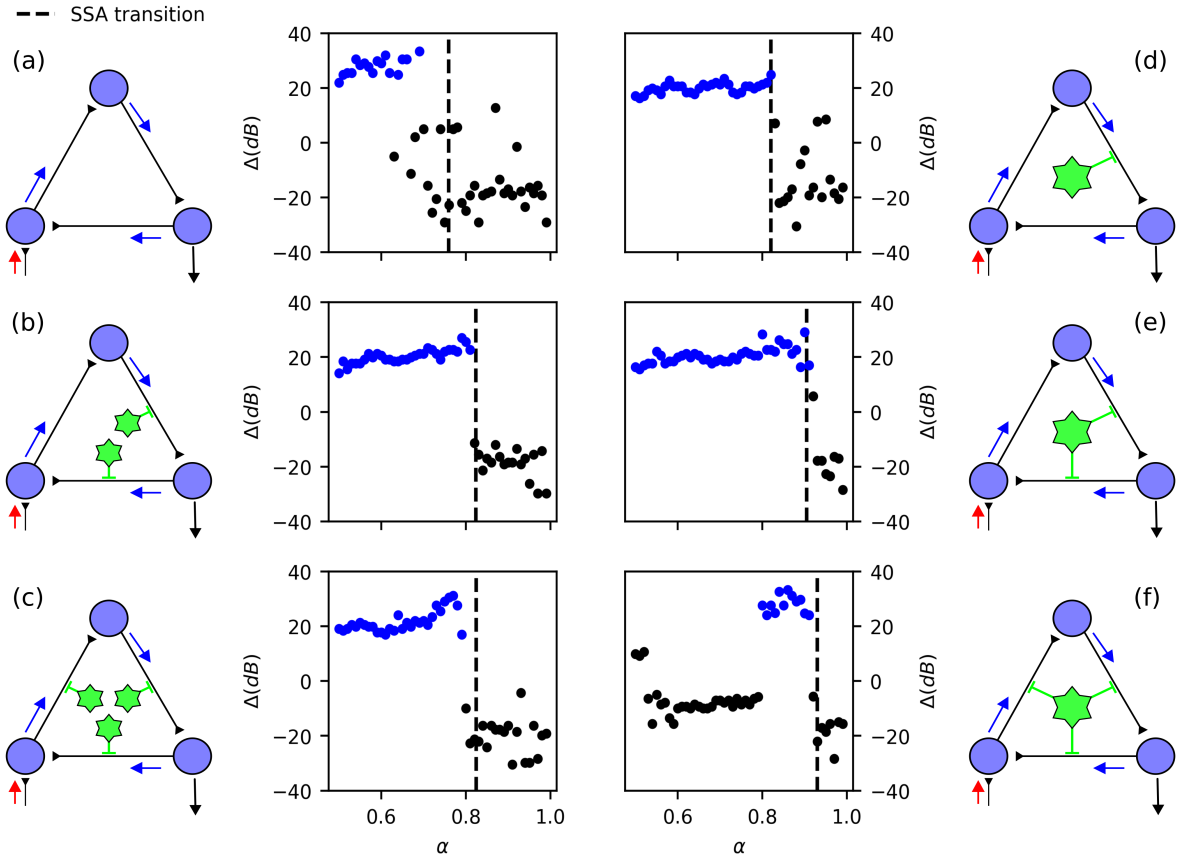

Supplementary figure G: **Estimation of dynamical range of circuit under different astrocytic modulation schemes.** Dynamical range Δ (dB) calculated from empirical transfer functions for different values of α. Positive dynamical range are plotted in blue, while negative values are in black. Dashed vertical line indicates the values of α identified as transition to a self-sustained activity regime (SSA), which approximately coincide with the breaking monotonicity of the empirical transfer function leading to less consistent estimation of the dynamical range. Case (a) without astrocyte modulaton present the less consistent dynamical range values across α. While the case (e) with high-order astrocytic modulation of the two internal synapse (synapse activated by internal circuit activity) present the largest interval of α with consistent positive large dynamical range across the interval.

7 Comparing different values of $\varepsilon < U_{SE}$.

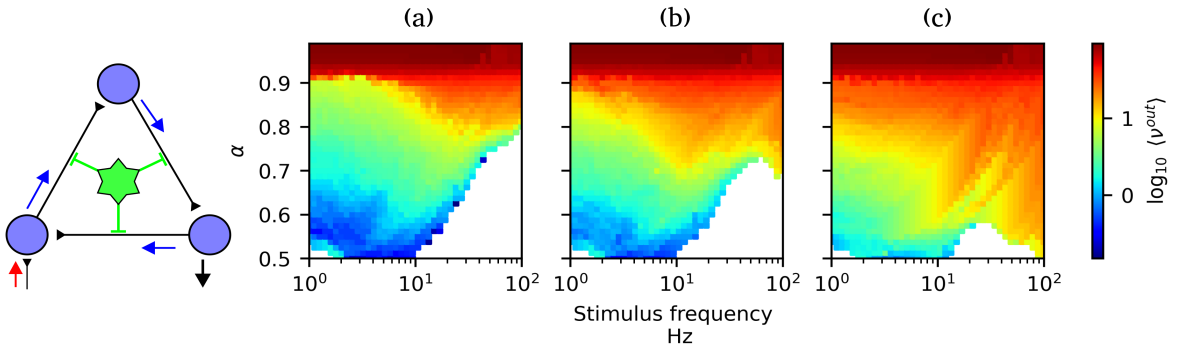

Supplementary figure H: **Comparison across different values of ε for $\varepsilon < U_{SE}$.** Firing rate of the read-out neuron ν^{out} as a function of the stimulation frequency and the parameter α for increasing values of ε: (a) $\varepsilon = 0.01$, (b) $\varepsilon = 0.05$, and (c) $\varepsilon = 0.09$. For all three simulations, $U_{SE} = 0.1$. As ε approaches U_{SE}, the modulatory effect of astrocytes decreases, since their contribution to synaptic facilitation scales with the factor $(\varepsilon - U_{SE})$. Consequently, the disruption of activity propagation to the read-out neuron (white regions in the heat maps), caused by excessive modulation, is progressively mitigated. However, even for $\varepsilon = 0.09$, a region of activity disruption is still observed.

8 Calcium integration and astrocyte modulation in different modulation schemes.

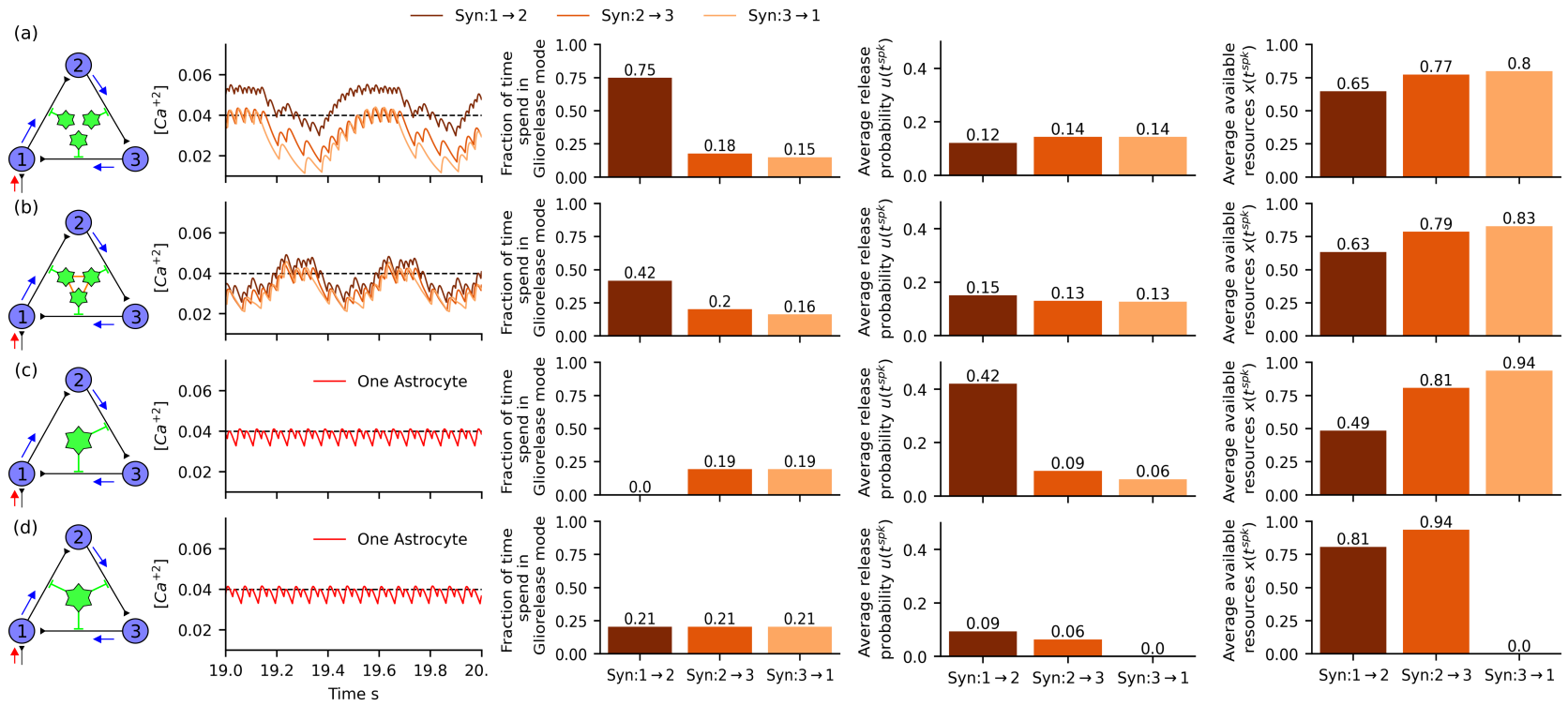

Supplementary figure I: **Calcium dynamics and astrocyte modulation across interaction schemes.** Each column shows: calcium concentration over time, gliorelease duration ($[Ca^{2+}] > Ca_{thr}$), average release probability, and available neurotransmitter resources at spike onset (t^{spk}). Rows correspond to modulation schemes: (a) Low-order via independent astrocytes; (b) Low-order with calcium diffusion ($D_{Ca} = 10^{-2}$); (c) High-order targeting internal synapses; (d) High-order including the external synapse ($1 \rightarrow 2$). In (a–b), astrocytes show large calcium fluctuations. The external synapse remains in gliorelease mode over 40% of the time, while others are active for less than half that. Diffusion in (b) reduces variability but has minimal effect on average modulation. High-order schemes (c–d) reduce calcium fluctuations via IP_3 integration in a single astrocyte, producing fewer but more effective gliorelease events. In (d), adding the external synapse increases gliorelease time slightly but disrupts activity propagation, silencing the read-out neuron (neuron 3). Stimulus firing rate equal to 30 Hz in all cases.

9 Clique size effect on activity

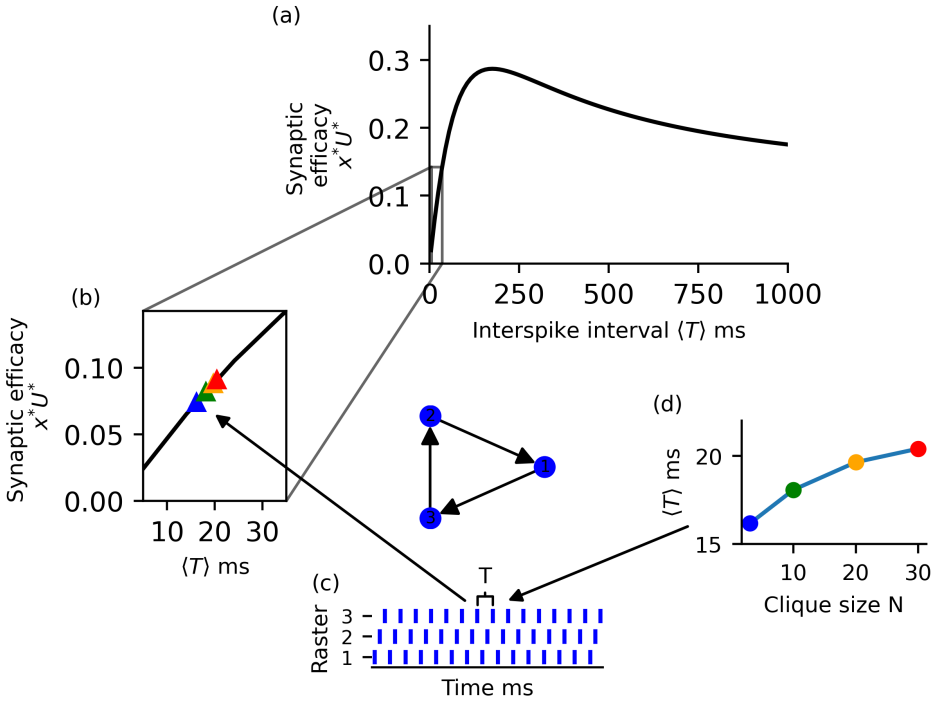

Supplementary figure J: **Synaptic efficacy as a function of clique size**. In the absence of gliotransmission, (a) the steady-state synaptic efficacy as a function of the pre-synaptic interspike interval can be computed analytically (black solid curve). (b) Synaptic efficacy increases with interspike interval—that is, it decreases with firing frequency. (c) Spike train (raster plot), when the neuronal clique is driven by recurrent activity, the interspike interval corresponds to the time T required for activity to propagate through the entire loop, completing one full cycle. (d) As the size of the clique increases, this propagation time also increases (blue solid curve in the inset), leading to longer interspike intervals. As a result, synaptic efficacy rises with clique size, enhancing recurrent excitation (increase synaptic current) and increasing the vulnerability of the network to enter a self-sustained activity (SSA) regime. Marker's color code correspond to data for different clique size N.

References

[1] M. Tsodyks, K. Pawelzik, and H. Markram, "Neural networks with dynamic synapses," *Neural Computation*, vol. 10, pp. 821–835, 5 1998.

[2] H. Markram and M. Tsodyks, "Redistribution of synaptic efficacy between neocortical pyramidal neurons," *Nature*, vol. 382, pp. 807–810, 8 1996.

[3] M. D. Pittà and N. Brunel, "Multiple forms of working memory emerge from synapse–astrocyte interactions in a neuron–glia network model," *Proceedings of the National Academy of Sciences*, vol. 119, 10 2022.